nrap

National Risk
Assessment Partnership

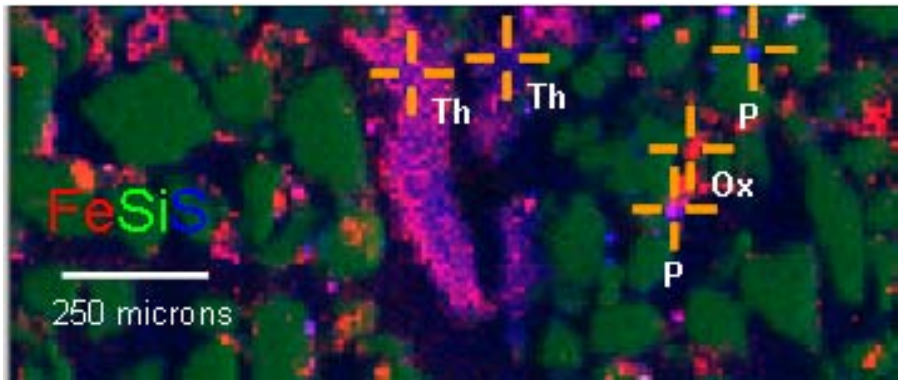

Laboratory and Synchrotron Analysis of Metal Sediment Associations

17 October 2012

U.S. DEPARTMENT OF ENERGY

NETL

Office of Fossil Energy

NRAP-TRS-III-003-2012

Disclaimer

This report was prepared as an account of work sponsored by an agency of the United States Government. Neither the United States Government nor any agency thereof, nor any of their employees, makes any warranty, express or implied, or assumes any legal liability or responsibility for the accuracy, completeness, or usefulness of any information, apparatus, product, or process disclosed, or represents that its use would not infringe privately owned rights. Reference therein to any specific commercial product, process, or service by trade name, trademark, manufacturer, or otherwise does not necessarily constitute or imply its endorsement, recommendation, or favoring by the United States Government or any agency thereof. The views and opinions of authors expressed therein do not necessarily state or reflect those of the United States Government or any agency thereof.

Cover Illustration: The distribution of iron, silicon and sulfur in a thin-section sample of the organic rich sediment.

Suggested Citation: Varadharajan, C.; Tinnacher, R.; Nico, P.S.; Zheng, L. *Laboratory and Synchrotron Analysis of Metal Sediment Associations*; NRAP-TRS-III-003-2012; NRAP Technical Report Series; U.S. Department of Energy, National Energy Technology Laboratory: Morgantown, WV, 2012; p 20.

An electronic version of this report can be found at: www.netl.doe.gov/nrap.

Laboratory and Synchrotron Analysis of Metal Sediment Associations

Charuleka Varadharajan[1], Ruth Tinnacher[1], Peter S. Nico[1], and Liange Zheng[1]

[1]Earth Sciences Division, Lawrence Berkeley National Laboratory, 1 Cyclotron Road Berkeley, CA 94720

NRAP-TRS-III-003-2012

Level III Technical Report Series

17 October 2012

This page intentionally left blank

Table of Contents

1. INTRODUCTION.....1

2. EXPERIMENTAL METHODS AND ANALYSES 2
2.1 MATERIALS EXAMINED 2
2.2 SELECTIVE EXTRACTIONS AND CARBON ANALYSIS 2
2.3 SYNCHROTRON ANALYSIS OF SEDIMENTS 2
2.4 SEQUENTIAL LEACHING TESTS 3
2.5 PRESSURIZED REACTOR CELL EXPERIMENTS.....3
2.6 BATCH EXPERIMENTS: PH-DRIVEN METAL RELEASE FROM SEDIMENTS...3

3. SUMMARY OF SEQUENTIAL EXTRACTION RESULTS 5
3.1 CARBON ANALYSIS.....5
3.2 SELECTIVE EXTRACTIONS 5

4. RESULTS OF METAL SEDIMENT ASSOCIATIONS FROM SYNCHROTRON ANALYSIS 6
4.1 BULK XAS SULFUR AND IRON ANALYSES.....6
4.2 ANALYSIS BY X-RAY MICROPROBE - MAJOR ELEMENT CHEMISTRY.....7
4.3 MICROPROBE ANALYSIS - CONTAMINANT ASSOCIATION.....8
4.4 SEQUENTIAL LEACHING WITH ELEVATED CO_2 AS COMPARED TO SIMPLE PH ADJUSTMENT 9

5. SUMMARY 13

6. REFERENCES.....14

List of Figures

Figure 1: Sulfur bulk-XANES spectra of the two sediment types. The vertical lines (L to R, increasing order of energy) represent the pyrite, thiosulfate (outer S), thiol, thiosulfate (inner S) and sulfate peaks respectively. 6

Figure 2: Iron, sulfur and silicon map of sandy sediment. Specks of pyrite (pink dots) were found, though most of the iron was associated with phyllosilicate clays. 7

Figure 3: The distribution of iron, silicon and sulfur in a thin-section sample of the organic rich sediment. 7

Figure 4: Sulfur XANES for spots “Th” & “P” in the organic rich sediment. 8

Figure 5: Fe XANES for locations (a) “P” and (b) “Ox” in the high organic matter sediment. 8

Figure 6(a): Major cations leached from the sandy sediment at 70psi CO_2 (red) or N2 (green) for 1, 4, 11 and 25 days. 10

Figure 6(b): Major cations leached from organic rich sediment at 70psi CO_2 (red) or N2 (green) for 1, 4, 11 and 25 days. 10

Figure 7: Comparison of metals released at elevated CO_2 between the sandy sediment (red) and the high organic matter sediment (blue) for 1, 4, 11 and 25 days. 11

Figure 8: Comparison of Mg and Mn release under elevated CO_2 concentrations and under simple pH adjustment concentrations. Data show release very similar between the two conditions for 1, 4, 11 and 25 days. 11

Figure 9: Comparison of Fe and Ca release under elevated CO_2 concentrations and under simple pH adjustment concentrations. Data show an impact of CO_2 for 1, 4, 11 and 25 days. 12

List of Tables

Table 1: Selective extraction results for the sandy sediment and high organic matter sediment. Comparison of results shows that significantly greater concentrations of trace metals were extract from the high organic matter sediment. 5

Acronyms and Abbreviations

Term	Description
EXAFS	Extended X-ray absorption fine structure
HOAc	Acetic acid
ICP-MS	Inductively coupled plasma mass spectrometry
LBNL	Lawrence Berkeley National Laboratory
psi	Pounds per square inch
PVC	Polyvinyl chloride
TIC	Total inorganic carbon
TOC	Total organic carbon
XANES	X-ray absorption near edge structure
XAS	X-ray absorption spectroscopy
XRD	X-ray diffraction

Acknowledgments

Portions of this work were completed as part of National Risk Assessment Partnership (NRAP) project. Support for this project came from the DOE Office of Fossil Energy's Crosscutting Research program. The authors wish to acknowledge Robert Romanosky (NETL Strategic Center for Coal) and Regis Conrad (DOE Office of Fossil Energy) for programmatic guidance, direction, and support.

NRAP funding was provided to Lawrence Berkeley National Laboratory (LBNL) under U.S. Department of Energy Contract No. DE-AC02-05CH11231. Additional funding for this study was provided by the U.S. Environmental Protection Agency, Office of Water and Office of Air and Radiation, under an Interagency Agreement with the U.S. Department of Energy, and by the Electric Power Research Institute, EPRI. The authors wish to thank Jeff Wagoner for developing the geologic framework model of the Southern San Joaquin Basin. Technical review by Marco Bianchi is greatly appreciated. Portions of this research were carried at the Advanced Light Source at LBNL, which is supported by the Director, Office of Science, Office of Basic Energy Sciences, of the U.S. Department of Energy under Contract No. DE-AC02-05CH11231. Portions of this research were carried out at the Stanford Synchrotron Radiation Lightsource, a Directorate of SLAC National Accelerator Laboratory and an Office of Science User Facility operated for the U.S. Department of Energy Office of Science by Stanford University.

1. INTRODUCTION

The risk of CO_2 leakage from properly characterized and permitted sequestration sites is expected to be low. However, CO_2 leakage into overlying groundwaters from deep storage sites has the potential to alter groundwater chemistry by increasing its acidity and dissolved carbonate content, which can subsequently result in the release of metals and ions that are naturally present in aquifer rocks and sediments (e.g., Apps et al., 2010; Zheng et al., 2009; Wang and Jaffe, 2004). Trace metals in sediments can be adsorbed on the surfaces of carbonates, iron (oxy)hydroxides and silicates, substituted in clay interlayers, coprecipitated in secondary carbonates, or present in trace quantities of host minerals. Reactions that can occur in the presence of elevated levels of CO_2 include processes such as dissolution of minerals such as carbonates (e.g., Kharakha et al., 2006; McGrath et al., 2007), sulfides (Apps et al., 2010) , or iron (oxy)hydroxides (Kharaka et al., 2006; 2009), ion exchange from clay interlayers (e.g., Zheng et al., 2012), desorption from mineral surfaces due to the increase of acidity (Zheng et al., 2009) as well as competitive desorption by competing carbonate ligands (Appelo et al., 2002). The kinetics of the different release mechanisms will vary, with ion-exchange and desorption likely occurring sooner than dissolution from host minerals.

This report describes results from laboratory work to help identify elements that can be mobilized in a potential leakage scenario, as well as to further understand the key geochemical reactions and transport processes that could lead to CO_2-induced release of metals. In addition to extensive sediment characterization conducted using a suite of laboratory and synchrotron techniques, a series of lab-scale leaching experiments with various degrees of difficulty were carried out to characterize metal release behavior in the presence and absence of elevated CO_2 concentrations under *in situ* conditions. The results from the more complex experiments involving reactor cells where sediments were exposed to CO_2-saturated solutions at formation pressures and redox conditions are compared against relatively simple pH adjustment experiments and selective extractions to identify potential screening protocols for site selection. The latter experiments aid in understanding the effects of pH-driven metal release as opposed to carbonate-driven metal release, and could enable us to evaluate the risk posed to groundwaters by a CO_2 leak using cost-effective and less time-consuming procedures.

2. EXPERIMENTAL METHODS AND ANALYSES

2.1 MATERIALS EXAMINED

Two distinct types of shallow-aquifer sediment materials were examined that differed primarily in their sand and organic matter content. The higher sand material is referred to as "sandy sediment" while the higher organic matter material is referred to as "high organic matter" sediment. The sediments were taken from an aquifer located at Jackson County, Mississippi where a field test of controlled release of dissolved CO_2 into a shallow groundwater aquifer was conducted (Trautz et al., 2012).

2.2 SELECTIVE EXTRACTIONS AND CARBON ANALYSIS

A series of selective extraction procedures were conducted to understand metal release under different leaching conditions and to assess the nature of metal-sediment associations. Extractions were conducted in parallel as opposed to sequentially in order to avoid alterations in chemical form from earlier extraction procedures. A series of major elements were analyzed for as shown in Table 1.

The functional fractions examined through these extractions include metals that were:

1. **Carbonates:** fraction bound to or precipitated as carbonate minerals [1 g dry sediment in 20 ml of 1 M NaAcetate-HOAc buffer adjusted to pH 5, shaken for 5 hours]
2. **Crystalline iron and manganese oxides**: fraction associated with higher range, low solubility Fe and Mn (hydr)oxides [1 g dry sediment in 30 ml of 1 M hydroxylamine hydrochloride in 25% (v/v) HOAc, heated at 95±5ºC for 6 hours]
3. **Total oxidizable:** fraction associated with minerals which dissolve under oxidizing conditions, largely metal sulfides and pyrite [1 g dry sediment in 25 ml of 0.17M potassium persulfate in 0.2% (v/v) H_2SO_4, heated at 95±5ºC for 1 hour]
4. **Amorphous sulfide phases:** fraction associated with amorphous metal sulfide phases [1 g dry sediment in 25 ml of 6 M HCl, shaken for 1 hour]
5. **Total carbon (TC) and total inorganic carbon (TIC):** measured using the solid-state module of a TIC - total organic carbon (TOC) analyzer equipped with an infra-red sensor (Shimadzu, SSM-5000A). Total carbon was measured by combusting ~ 500 mg of sample at 1000ºC. Total inorganic carbon was measured by acidifying ~500 mg of sample with 85% phosphoric acid, followed by combustion at 250ºC. The total organic carbon fraction was determined as the difference between the TC and TIC measurements.

2.3 SYNCHROTRON ANALYSIS OF SEDIMENTS

Both bulk and microfocused X-ray Absorption Spectroscopy (XAS) synchrotron analysis were conducted. Bulk S and Fe XAS analysis was conducted at beamline 4-3 of the Stanford Synchrotron Radiation Laboratory. Microfocused XAS was done at the beamline 10.3.2 of the Advanced Light Source at Lawrence Berkeley National Laboratory.

2.4 SEQUENTIAL LEACHING TESTS

Laboratory experiments were carried out to evaluate metal release from the sediments under the low-pH conditions (pH~5) expected when elevated CO_2 concentrations occur in the groundwater. Two different types of experimental setups were used—(1) pressurized reactor-cell experiments using synthetic groundwater saturated with CO_2, and (2) batch systems using pH-adjusted, synthetic groundwater equilibrated with a CO_2-free atmosphere. For both types of systems, additional control experiments with synthetic groundwater were performed to mimic metal release behavior at *in situ* pH conditions (pH~8.5) for comparison. A total of three different sediments—two from the sandy sediment (sandy sediment 1 and sandy sediment 2), and one from the high organic matter sediment were used in the experiments in order to identify the effects of different sediment on metal release behavior.

In these sequential leaching experiments, the sediments were initially brought into contact with the groundwater solutions, then were repeatedly exchanged after equilibration with solids over four successive time-frames of 1, 4, 11 and 25 days as in a series of stop-flow events with increasing residence times. The cell solutions were analyzed for their solute composition at each of the four time-points. The synthetic groundwater used was similar in composition to the water at the field site (Trautz et al., 2012), comprising of 6.4 mM $NaHCO_3$, 0.7 mM NaCl, 0.1 mM KCl, 0.1 mM $CaCl_2$, and 0.3 mM Na acetate (intended as a substitute for various organics). Samples for cations were preserved using 2% (v/v) ultra high purity nitric acid and were analyzed by ICP-MS (Perkin-Elmer SCIEX ICP-Mass Spectrometer ELAN DRC II). All chemicals used in the experiments were reagent grade or better. Aqueous solutions were prepared with Milli-Q water (Millipore Elix 10 UV system), and all glassware was acid washed prior to use.

2.5 PRESSURIZED REACTOR CELL EXPERIMENTS

Miniature pressurized reaction cells were used to independently test the release of metals under elevated dissolved CO_2 concentrations and realistic aquifer pressures from heterogeneous sediment materials. Three grams of sediments were exposed in custom-made PVC reactor cells to ~ 15 ml of synthetic groundwater saturated with CO_2 gas at the pressure at the average depth of the target formation (Trautz et al., 2012) (70-80 psi / 4.8 – 5 bar, pH 5). In addition, the sediments were separately subject to N_2-sparged synthetic groundwater at 70-80 psi and pH 8.5 to evaluate baseline metal release under the reducing conditions present in the target formation. Duplicates of sediments and blanks were included with each test. All fittings and components of the setup were acid-washed prior to use and cell solutions were collected in trace-metal clean centrifuge vials (VWR Scientific) during sampling. The solutions were sparged for ~ 3 days in the reservoir prior to the start of the experiment. The sequential leaching stop-flow experiments involved sampling the cells at intervals of 1, 4, 11 and 25 days, followed by a refill with fresh influent solution.

2.6 BATCH EXPERIMENTS: PH-DRIVEN METAL RELEASE FROM SEDIMENTS

Batch experiments were set up at room temperature in a CO_2-free atmosphere using a glove box filled with mixed gas (93.3%N_2, 5.7% H_2). At the beginning of the experiment, 3.75 g of sediment were weighed into 50 mL trace-metal clean centrifuge tubes, to which 15 mL of synthetic groundwater solution at the specified pH was added. In addition, control vials were set up containing the same synthetic groundwater solutions but without any sediment. These

controls allowed for the monitoring of potential changes in solution pH and groundwater composition over the course of the experiment, e.g., due to precipitation reactions or loss of inorganic carbon. All sediment samples and controls were prepared in duplicates. Lastly, a control vial (one replicate) containing the same volume of Milli-Q water was set up in order to measure variations in solution temperatures during the experiment (22.5 – 23.5°C), and to confirm that sample centrifugation did not cause any increase in solution temperatures.

After recording the exact weights of sediments in each sample vial, 15-mL aliquots of pH-adjusted synthetic groundwater solutions were added. Then, vial caps were wrapped with parafilm and set up on a Thermo Scientific Rotator shaker to facilitate metal release reactions from sediments under ideal mixing conditions. The exact starting time of the shaking period was recorded. After specified time-frames, which were comparable to the sediment-solution contact times used in flow-cell experiments (20.5 hours, 4, 11 and 25 days), the shaking of samples was interrupted, and supernatant solutions were sampled and replaced with fresh groundwater solutions.

3. SUMMARY OF SEQUENTIAL EXTRACTION RESULTS

3.1 CARBON ANALYSIS

The organic rich sediment contained 2.4% by weight total carbon, all of which was organic matter. The rest of the sandy sediment contained less than 0.01% total carbon. The results were not affected by changes to initial moisture content or crushing of the sediments.

3.2 SELECTIVE EXTRACTIONS

Table 1 shows the results of selective extractions performed on the sand as well as the black lamination material. Table 1 shows the rough category of sediment material targeted by the extraction and the conditions used. For all cases, there were significantly greater concentrations of metals extracted from the high organic matter sediment than from the sandy sediment. Significant quantities of Ca, Mg, and Sr were extracted under the mild acetic acid (HOAc) at pH =5 conditions (extraction 1) indicting that these materials were either bonded in trace carbonates or on easily exchangeable sites. Both the high organic matter and sandy sediment showed release of Fe as a result of persulfate oxidation (extraction 3) confirming the presence of pyrite as indicated by the XRD and XAS.

Taken together the sediment characterization results show that the sandy sediment is a quartz based sand coated and interspersed with small amounts of Fe containing phylloscilitate clays, Fe (hydr)oxides, amorphous FeS, and pyrite (Varadharajan et al., 2012). The presence of the high organic matter sediment and the FeS and pyrite indicate a generally reducing environment. The selective extractions show that under the mild acetic conditions expected due to the CO_2 injection significant quantities of divalent cations, e.g., Ca, Mg, Sr, and Mn, will likely be released either via cation exchange or dissolution of trace carbonates. The release of metals and metalloids of more environmental concern is possible if dissolution of FeS or pyrite occur as these grains were identified to contain As and some fraction of Pb.

Table 1: Selective extraction results for the sandy sediment and high organic matter sediment. Comparison of results shows that significantly greater concentrations of trace metals were extract from the high organic matter sediment.

Extraction Target and Method		Sandy Sediment (µg/g) (values are average of four measurements with standard deviations shown)					High Organic Matter Sediment (µg/g) (due to sample limitation values are single measurements)				
		Ca	Mg	Sr	Mn	Fe	Ca	Mg	Sr	Mn	Fe
1	**Carbonates**	113 (19)	50 (6)	3.9 (0.5)	2.3 (0.2)	9.8 (2)	867	275	28	36	21
2	**Crystalline iron and manganese oxides**	130 (47)	73 (36)	4.8 (0.5)	3.5 (0.4)	119 (62)	820	265	24	30	755
3	**Total oxidizable**	105 (15)	63 (50)	3.6 (0.8)	1.4 (1.3)	218 (130)	755	212	16	8	813
4	**Amorphous sulfide phases**	101 (14)	46 (19)	3.1 (0.5)	2.8 (0.6)	98 (46)	749	210	16	29	232

4. RESULTS OF METAL SEDIMENT ASSOCIATIONS FROM SYNCHROTRON ANALYSIS

4.1 BULK XAS SULFUR AND IRON ANALYSES

The results of the sulfur analysis are show in Figure 1. All three materials contain reduced sulfur species as shown by the peaks in the 2472 – 2475 eV range. The sulfur speciation in the sandy sediment is dominated by sulfate, which is consistent with the $CaSO_4$ found in the sediment characterization conducted by Southern Co. Smaller amounts of reduced sulfur species are also present, and include pyrite (FeS_2), thiosulfate ($S_2O_3^{2-}$), and potentially organic thiol groups (R-SH groups). In contrast, the sulfur in the organic rich sediment is mostly in the form of organic thiol groups, which is consistent with the morphology observed with the light microscope as well as the high organic C measurements mentioned above.

The results from linear combination fitting of the iron extended X-ray absorption fine structure (EXAFS) spectra indicate that the bulk aquifer material mostly consisted of iron-bearing clays and silicates, Fe-oxides, and to lesser extent sulfides. In contrast, a larger fraction of the iron in the high organic matter sediment was associated with sulfides (mainly pyrite). The rest of the iron in this layer was present as Fe-oxides and silicates. The transition zone mainly consisted of Fe-oxides and iron-bearing silicates and clays. A small amount of pyrite was seen in this zone.

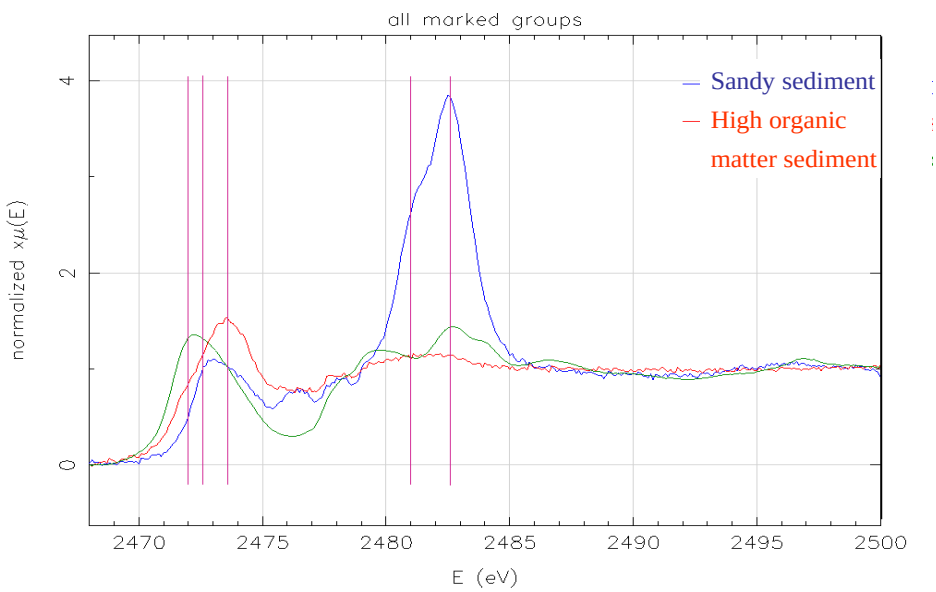

Figure 1: Sulfur bulk-XANES spectra of the two sediment types. The vertical lines (L to R, increasing order of energy) represent the pyrite, thiosulfate (outer S), thiol, thiosulfate (inner S) and sulfate peaks respectively.

4.2 ANALYSIS BY X-RAY MICROPROBE - MAJOR ELEMENT CHEMISTRY

A detailed analysis of thin sections of the sandy sediment and high organic matter sediment was done at beamline 10.3.2 of the Advanced Light Source (a hard X-ray microprobe). Figure 2 shows an iron, silicon, sulfur map of the sandy sediment; the image shows the sample consists largely of silicon-rich grains that were identified as quartz with the light microscope. The iron in the sample was dominated by iron-bearing phyllosilicate clays, and also contained minor amounts of Fe (hydr)oxides. A few sulfur and iron-rich grains were present and were identified as pyrite (pink dots in Figure 2).

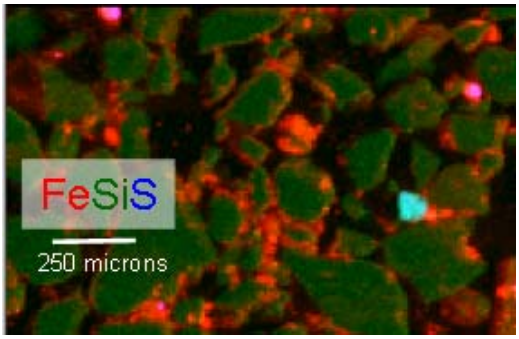

Figure 2: Iron, sulfur and silicon map of sandy sediment. Specks of pyrite (pink dots) were found, though most of the iron was associated with phyllosilicate clays.

Microprobe analysis of the organic-rich sediment shows a similar quartz dominated matrix (Figure 3). The sample also contained large amorphous sulfur-rich material associated with a significant amount of iron (e.g., around spots marked “Th”), small iron and sulfur-rich grains (e.g., spots marked “P”), as well as patches of iron-rich material (e.g., spot marked “Ox”).

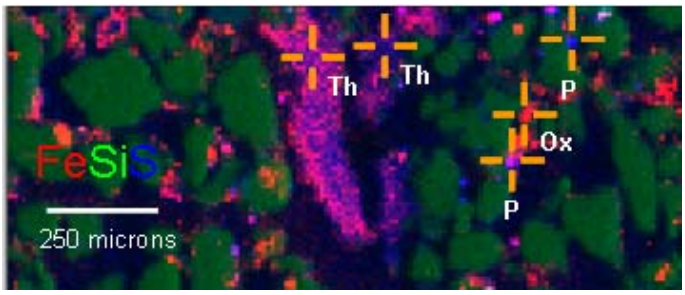

Figure 3: The distribution of iron, silicon and sulfur in a thin-section sample of the organic rich sediment.

The sulfur speciation at the two locations within the amorphous sulfur regions labeled “Th” was dominated by thiol groups (Figure 3). In contrast, the small, dense sulfur grains, labeled “P”, were found to be pyrite. The presence of pyrite (FeS_2) at these locations was confirmed by linear combination fitting of the Fe X-ray absorption near edge structure (XANES) spectra (Figure 4), though some amount of FeS could also be present (Figure 5a). In contrast, the iron at the location labeled “Ox” was mainly present in the form of iron-bearing phyllosilicate clays (specifically illite), with a small amount of reduced iron species (Figure 5b).

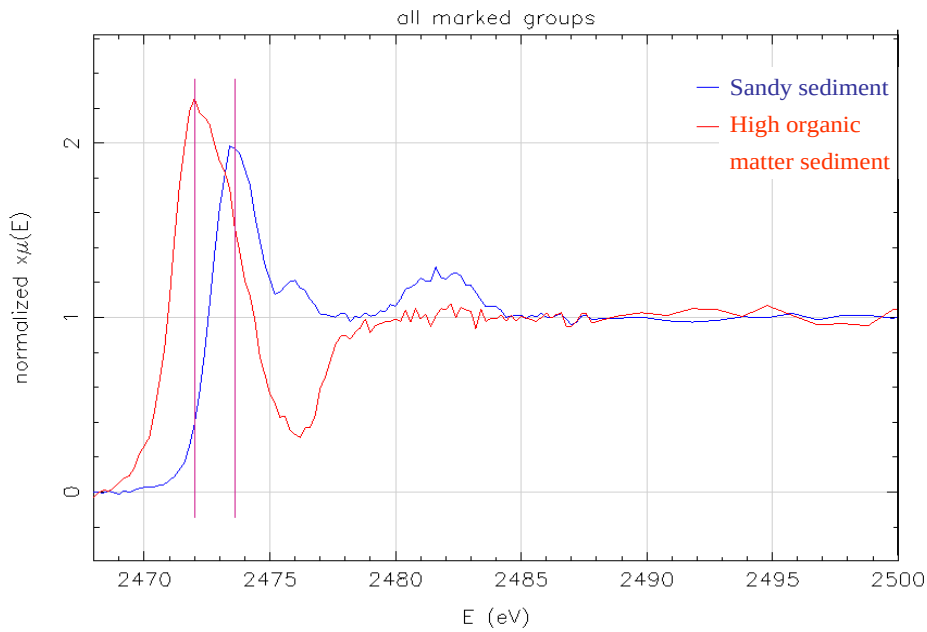

Figure 4: Sulfur XANES for spots "Th" & "P" in the organic rich sediment.

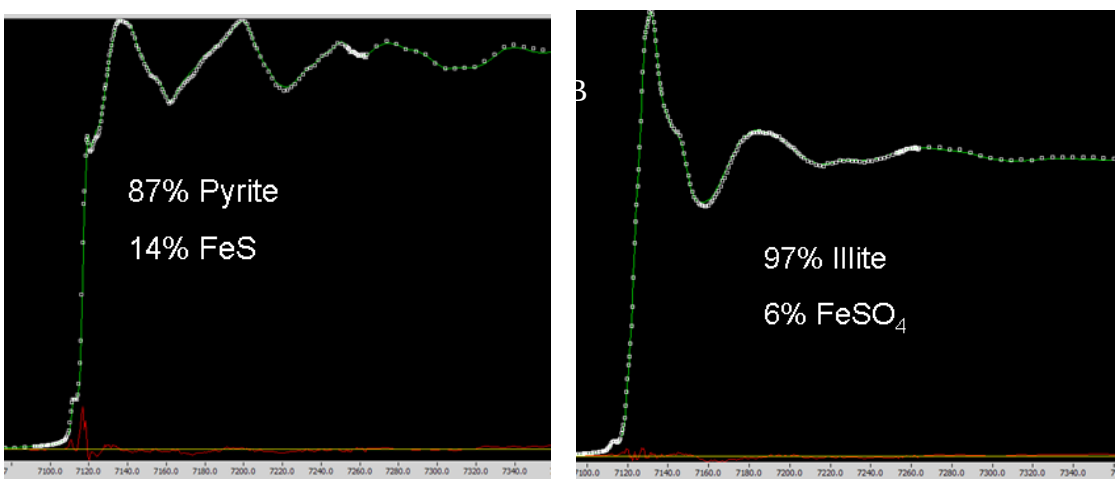

Figure 5: Fe XANES for locations (a) "P" and (b) "Ox" in the high organic matter sediment.

4.3 MICROPROBE ANALYSIS - CONTAMINANT ASSOCIATION

The association of potential contaminants with different phases within the high organic matter sediment and sandy sediment was determined by collecting X-ray fluorescence spectra at selected locations. Three classes of associations were noted. First, the pyrite grains contained inclusions of significant quantities of both arsenic and lead, as well as smaller amounts of selenium. Second, the iron-clay and iron-oxide regions were associated with elevated concentrations of strontium, rubidium, and chromium, as well as smaller amounts of lead and arsenic. Third, the major potential contaminant associated with the organic matter was

germanium. Some elevation in strontium and rubidium was also seen but this could be a result of the comingling of the iron-clays and oxides in the organic material.

4.4 SEQUENTIAL LEACHING WITH ELEVATED CO_2 AS COMPARED TO SIMPLE PH ADJUSTMENT

Figure 6(a) shows the results from the selective leaching of the sand sediment with elevated CO_2 groundwater for several major cations, Na, Mg, Fe, and Mn. The results show that there was greater release under conditions of elevated CO_2 as compared with the baseline experiments using N_2 at the same pressure. The release of all metals was relatively rapid with the greatest concentrations being seen after only one day of leaching. The rapid release kinetics favor the hypothesis that these metals were released via kinetically fast processes, such as desorption or ion exchange, as opposed to a kinetically more limited process such as dissolution. The fact that the concentrations of metals were lower for later time periods in spite of leaching time being greater strongly implies that the source of these metals was rapidly depleted. Figure 6(b) shows the same figure for the organic-rich sediment.

The release of Mg, Mn, As, and Ni from the two different sediment types under elevated CO_2 conditions is shown in Figure 7. The most dramatic result is that the degree of metal release at all time points is roughly an order of magnitude greater in the high organic matter sediment as compared to the sandy sediment. Interestingly, the general release profiles are similar in terms of the highest concentrations after a single day of leaching and decreasing concentrations at later times.

Finally, the comparison between the metal release due to elevated CO_2 conditions and due to a simple pH adjustment is shown in Figures 8 and 9. In Figure 8, it is shown that Mg shows very similar behavior between tests featuring simple HCl pH adjustment compared to elevated CO_2 conditions, indicating that there is only a minor impact of the CO_2 itself (i.e., Mg release is mostly driven by the pH change). Similar results were seen for Sr, Na, K, and Ba. While Mn appears to be mostly impacted by the pH change, there is a slight enhancement of release under elevated CO_2 conditions on day 1 and 4, but the difference appears to diminish with time. In Figure 9, it can be seem that for Fe and Ca the presence or absence of CO_2 can make a significant difference in the amount of metal released at different times. Thus, here the main driver for Fe and Ca release appears to be the impact of dissolved CO_2 itself rather than the pH change.

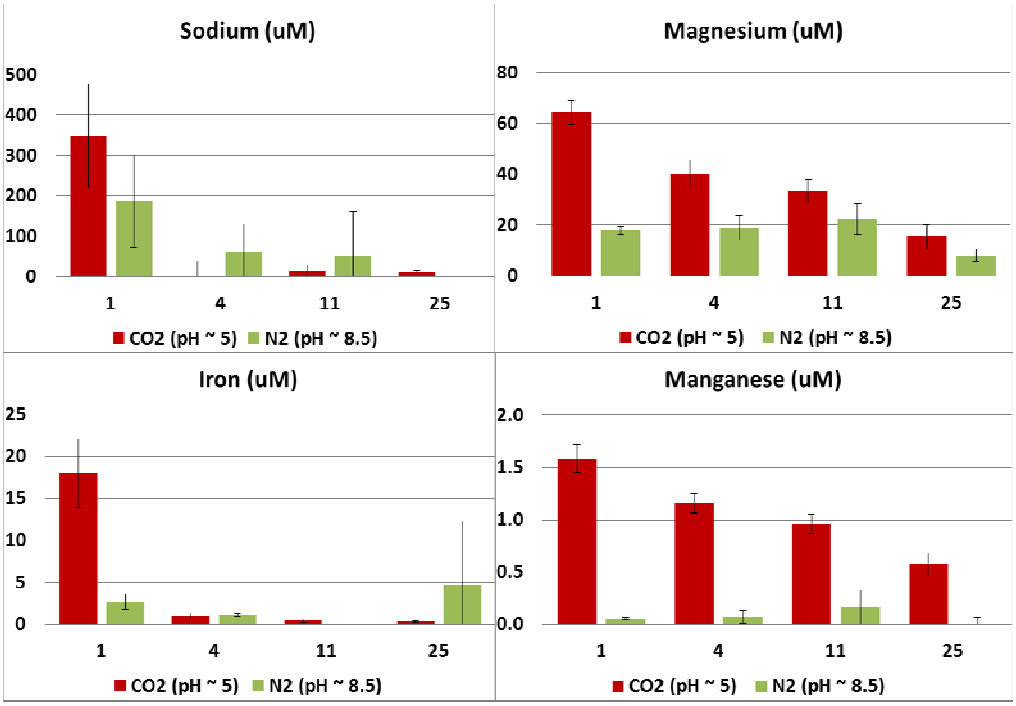

Figure 6(a): Major cations leached from the sandy sediment at 70psi CO_2 (red) or N2 (green) for 1, 4, 11 and 25 days.

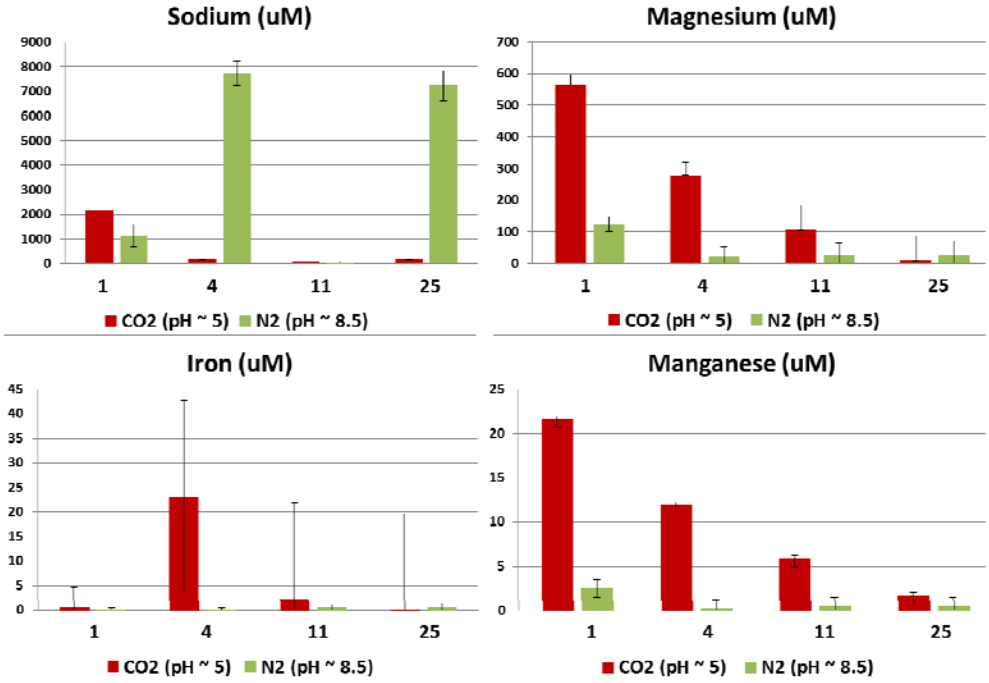

Figure 6(b): Major cations leached from organic rich sediment at 70psi CO_2 (red) or N2 (green) for 1, 4, 11 and 25 days.

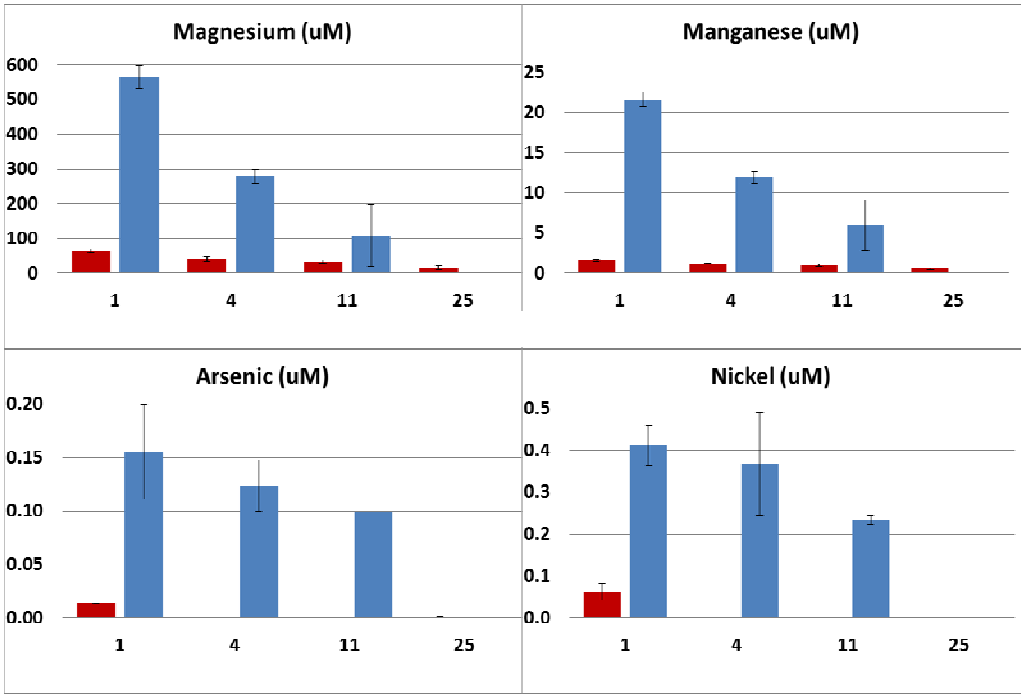

Figure 7: Comparison of metals released at elevated CO_2 between the sandy sediment (red) and the high organic matter sediment (blue) for 1, 4, 11 and 25 days.

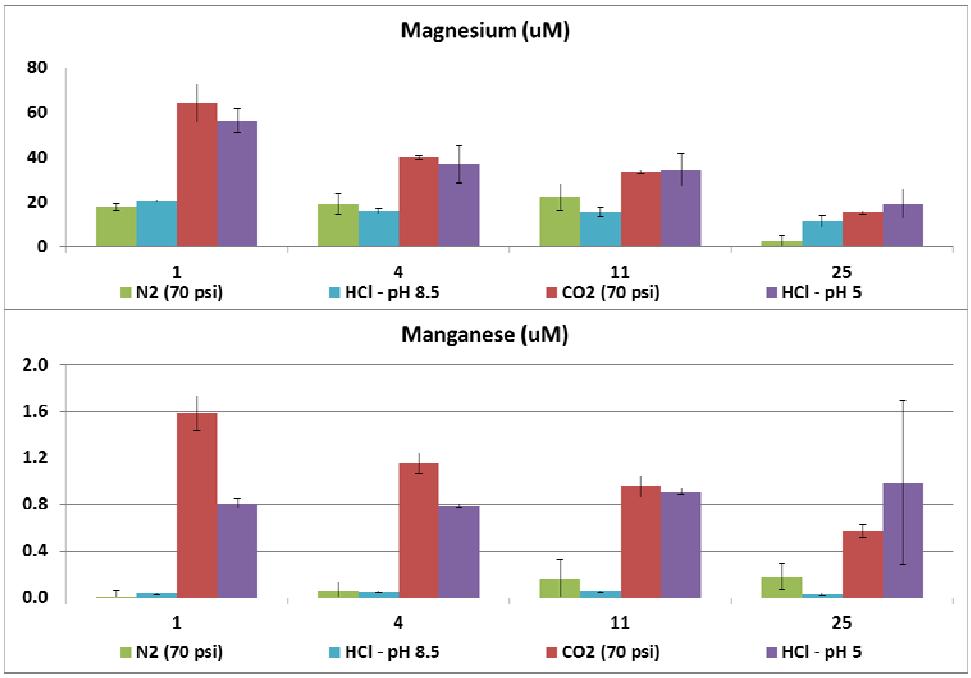

Figure 8: Comparison of Mg and Mn release under elevated CO_2 concentrations and under simple pH adjustment concentrations. Data show release very similar between the two conditions for 1, 4, 11 and 25 days.

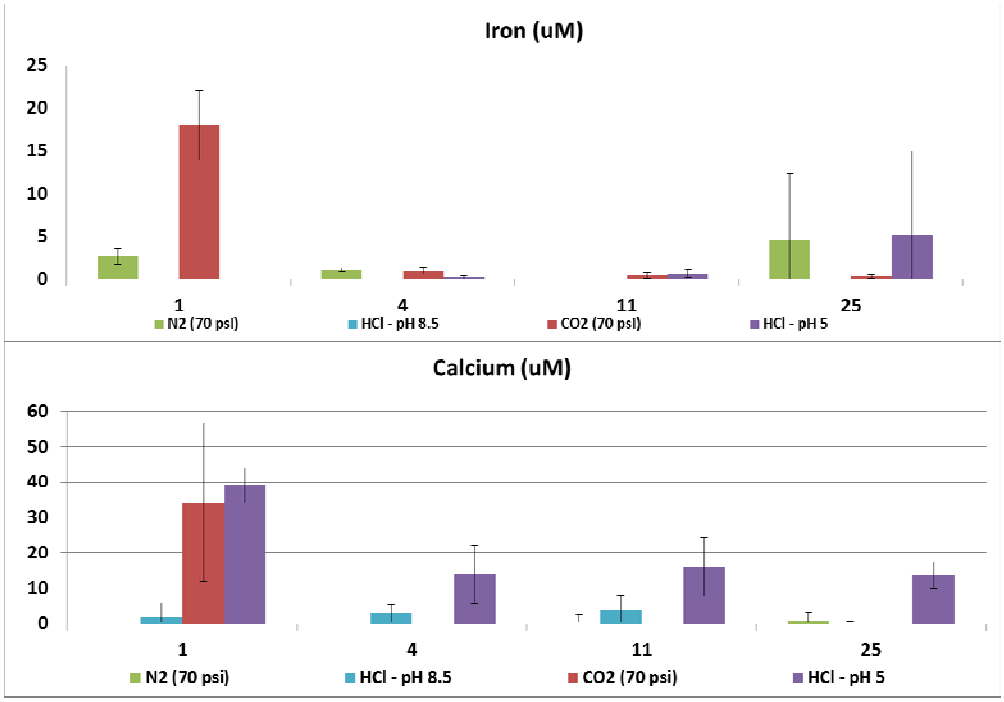

Figure 9: Comparison of Fe and Ca release under elevated CO_2 concentrations and under simple pH adjustment concentrations. Data show an impact of CO_2 for 1, 4, 11 and 25 days.

5. SUMMARY

Core materials from two aquifer sediments were analyzed: one relatively low in metals and dominated by sand (sandy sediment), the other with relatively high organic carbon and high metal content (high organic matter sediment). The results so far have shown that the sandy sediment contains large quartz grains, some of which are coated with iron-bearing clays and oxides. The material does not contain much carbon, and has a low buffering capacity. In contrast, the high organic matter sediment contains a significant amount of organic carbon (2.4%), which is likely present as organic thiol groups. Arsenic and lead were found to be associated with discrete pyrite grains in both sediments, though the sandy sediment has much smaller amounts of pyrite than the high organic matter sediment.

The sequential leaching experiments showed that the release of several metals, e.g., Mg, Sr, Na, K, Ba and to some extent Mn, was controlled almost exclusively by the change in pH and not the change in CO_2 concentrations. In contrast, Fe and Ca release were shown to be influenced not only by pH changes but also by CO_2 concentrations. For all the metals discussed here the magnitude of the release diminished rapidly in time, indicating quick release kinetics and a limited source of labile metal. The degree of metal release in the leaching experiments is roughly an order of magnitude greater in the high organic matter sediment as compared to the sandy sediment. Based on these results, the high organic matter sediment could be a more significant source of metals though the sandy sediment material is more abundant in the aquifer. Also, while the pyrite grains did contain elevated As and Pb, there were metals distributed across the clays and Fe oxides materials that could be released via desorption or ion exchange processes. The rapid pulse-like release of elements seen in the lab results is very similar to the pulse results seen in the controlled-release field experiment mentioned earlier (Trautz et al., 2012). This both supports the accuracy of the field observations and validates the lab approach as being useful for understanding or predicting field behavior. The fact that the simple pH adjustment extraction reproduced many of the major results of the more complicated elevated CO_2 extraction may mean that simple extractions of this type are suitable for helping to estimate risk of metal release in specific aquifers.

6. REFERENCES

Appelo, C. A. J.; Van Der Weiden, M. J. J.; Tournassat, C.; Charlet, L. Surface complexation of ferrous iron and carbonate on ferrihydrite and the mobilization of arsenic. *Environmental Science & Technology* **2002,** *36*(14), 3096-3103.

Apps, J. A.; Zheng, L.; Zhang, Y.; Xu, T.; Birkholzer, J. T. Evaluation of groundwater quality changes in response to CO_2 leakage from deep geological storage. *Transport in Porous Media* **2010,** *82*(1), 215-246.

Kharaka, Y. K.; Cole, D. R.; Hovorka, S. D.; Gunter, W. D.; Knauss, K. G.; Freifeld, B. M. Gas-water-rock interaction in Frio formation following CO_2 injection: implications for the storage of greenhouse gases in sedimentary basins. *Geology* **2006,** *34*, 577-580.

Kharaka, Y. K.; Thordsen, J. J.; Hovorka, S. D.; Nance, S.; Cole, D. R.; Phelps, T. J.; Knauss, K. G. Potential environmental issues of CO_2 storage in deep saline aquifers: Geochemical results from the Frio-I brine pilot test, Texas, USA. *Applied Geochemistry* **2009,** *24*, 1106-1112.

McGrath, A. E., Upson, G. L. and Caldwell, M. D. Evaluation and mitigation of landfill gas impacts on cadmium leaching from native soils. *Ground Water Monitoring & Remediation* **2007,** *27*, 99-109.

Trautz, R.C.; Pugh, J.D.; Varadharajan, C.; Zheng, L.; Bianchi, M.; Nico, P.S.; Spycher, N.F.; Newell, D.L.; Esposito, R.A.; Wu, Y.; Dafflon, B.; Hubbard, S.S.; Birkholzer, J.T. Effect of dissolved CO_2 on a shallow groundwater system: a controlled release field experiment. *Environmental Science & Technology* **2012,** in press.

Varadharajan, C.; Birkholzer, J.T.; Esposito, R.; Nico, P.; Pugh, J.; Spycher, N.; Trautz, R.; Zheng, L. Effects of dissolved CO_2 on mobility of naturally occurring trace metals in groundwater using laboratory leaching experiments. *11th Annual Conference on Carbon Capture, Utilization and Sequestration,* Pittsburgh, PA, April 30 – May 3, 2012.

Wang, S.; Jaffe, P. R. Dissolution of a mineral phase in potable aquifers due to CO_2 releases from deep formations; effect of dissolution kinetics. *Energy Conversion and Management* **2004,** *45*, 2833-2848.

Zheng, L.; Apps, J. A.; Zhang, Y.; Xu, T.; Birkholzer, J. T. On mobilization of lead and arsenic in groundwater in response to CO_2 leakage from deep geological storage. *Chemical Geology* **2009,** *268*(3-4), 281-297.

Zheng, L.; Apps, J. A.; Spycher, N.; Birkholzer, J. T.; Kharaka, Y. K.; Thordsen, J.; Beers, S. R.; Herkelrath, W. N.; Kakouros, E.; Trautz, R. C. Geochemical modeling of changes in shallow groundwater chemistry observed during the MSU-ZERT CO_2 injection experiment. *International Journal of Greenhouse Gas Control* **2012,** *7*(0), 202-217.

nrap
National Risk
Assessment Partnership

NRAP is an initiative within DOE's Office of Fossil Energy and is led by the National Energy Technology Laboratory (NETL). It is a multi-national-lab effort that leverages broad technical capabilities across the DOE complex to develop an integrated science base that can be applied to risk assessment for long-term storage of carbon dioxide (CO_2). NRAP involves five DOE national laboratories: NETL-RUA, Lawrence Berkeley National Laboratory (LBNL), Lawrence Livermore National Laboratory (LLNL), Los Alamos National Laboratory (LANL), and Pacific Northwest National Laboratory (PNNL). The NETL-RUA is an applied research collaboration that combines NETL's energy research expertise in the Office of Research and Development (ORD) with the broad capabilities of five nationally recognized, regional universities—Carnegie Mellon University (CMU), The Pennsylvania State University (PSU), the University of Pittsburgh (Pitt), Virginia Tech (VT), and West Virginia University (WVU)—and the engineering and construction expertise of an industry partner (URS Corporation).

NRAP Technical Leadership Team

Jens Birkholzer
LBNL Technical Coordinator
Lawrence Berkeley National Laboratory
Berkeley, CA

Grant Bromhal
NETL Technical Coordinator
Lead, Reservoir Working Group
Office of Research and Development
National Energy Technology Laboratory
Morgantown, WV

Chris Brown
PNNL Technical Coordinator
Lead, Groundwater Working Group
Pacific Northwest National Laboratory
Richmond, WA

Susan Carroll
LLNL Technical Coordinator
Lawrence Livermore National Laboratory
Livermore, CA

Laura Chiaramonte
Lead, Natural Seals Working Group
Lawrence Livermore National Laboratory
Livermore, CA

Tom Daley
Lead, Monitoring Working Group
Lawrence Berkeley National Laboratory
Berkeley, CA

George Guthrie
Technical Director, NRAP
Office of Research and Development
National Energy Technology Laboratory
Pittsburgh, PA

Rajesh Pawar
LANL Technical Coordinator
Lead, Systems Modeling Working Group
Los Alamos National Laboratory
Los Alamos, NM

Tom Richard
Deputy Technical Director, NRAP
The Pennsylvania State University
NETL-Regional University Alliance
State College, PA

Brian Strazisar
Lead, Wellbore Integrity Working Group
Office of Research and Development
National Energy Technology Laboratory
Pittsburgh, PA

Sean Plasynski
Deputy Director
Strategic Center for Coal
National Energy Technology Laboratory
U.S. Department of Energy

Jared Ciferno
Director
Office of Coal and Power R&D
National Energy Technology Laboratory
U.S. Department of Energy

Robert Romanosky
Technology Manager
Office of Coal and Power R&D
National Energy Technology Laboratory
U.S. Department of Energy

Regis Conrad
Director
Division of Cross-cutting Research
Office of Fossil Energy
U.S. Department of Energy

NRAP Executive Committee

Cynthia Powell
Director
Office of Research and Development
National Energy Technology Laboratory
U.S. Department of Energy

Alain Bonneville
Laboratory Fellow
Pacific Northwest National Laboratory

Donald DePaolo
Associate Laboratory Director
Energy and Environmental Sciences
Lawrence Berkeley National Laboratory

Melissa Fox
Chair, NRAP Executive Committee
Program Manager
Applied Energy Programs
Los Alamos National Laboratory

Julio Friedmann
Chief Energy Technologist
Lawrence Livermore National
Laboratory

George Guthrie
Technical Director, NRAP
Office of Research and Development
National Energy Technology Laboratory

NRAP Technical Report Series